JOC*Article*

Assignment of the EPR Spectrum of 5,5-Dimethyl-1-pyrroline *N*-Oxide (DMPO) Superoxide Spin Adduct†

Jean-Louis Clément,‡ Nicolas Ferré,§ Didier Siri,§ Hakim Karoui,‡ Antal Rockenbauer,|| and Paul Tordo*,‡

UMR 6517, CNRS and Aix-Marseille Universities, Centre de Saint Jérôme, 13397 Marseilles, Cedex 20, France, and Chemical Research Center, Institute for Chemistry, P.O. Box 17, H-125 Budapest, Hungary

ptordo@srepir1.univ-mrs.fr

Received August 24, 2004

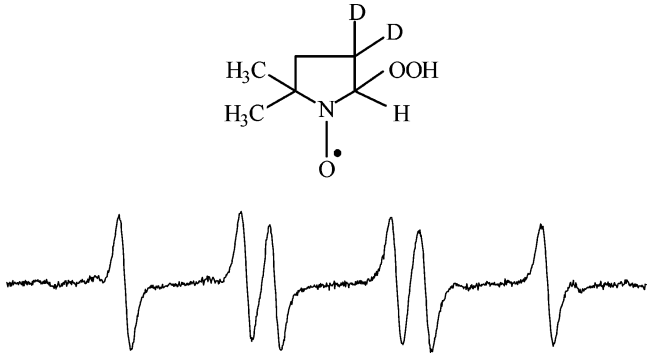

Spin trapping consists of using a nitrone or a nitroso compound to "trap" an unstable free radical as a long-lived nitroxide that can be characterized by electron paramagnetic resonance (EPR) spectroscopy. The formation of DMPO−OOH, the spin adduct resulting from trapping superoxide ($O_2^{\bullet-}$) with 5,5-dimethyl-1-pyrroline *N*-oxide (DMPO), has been exploited to detect the generation of superoxide in a wide variety of biological and chemical systems. The 12-line EPR spectrum of DMPO−OOH has been either reported or mentioned in more than a thousand papers. It has been interpreted as resulting from the following couplings: $A_N \simeq 1.42$ mT, $A_{H^\beta} \simeq 1.134$ mT, and A_{H^γ} (1H) $\simeq 0.125$ mT. However, the DMPO−OOH EPR spectrum has an asymmetry that cannot be reproduced when the spectrum is calculated considering a single species. Recently, it was proposed that the 0.125 mT splitting was misassigned and actually results from the superimposition of two individual EPR spectra associated with different conformers of DMPO−OOH. We have prepared 5,5-dimethyl-[3,3-$^2H_2$]-1-pyrroline *N*-oxide (DMPO-d_2), and we showed that the EPR spectrum of the corresponding superoxide spin adduct is composed of only six lines, in agreement with the assignment of the 0.125 mT splitting to a γ-splitting from a hydrogen atom bonded to carbon 3 of DMPO. This result was supported by DFT calculations including water solvation, and the asymmetry of the DMPO−OOH EPR spectrum was nicely reproduced assuming a chemical exchange between two conformers.

Introduction

Since the discovery[1] of superoxide dismutase (SOD), the role of superoxide ($O_2^{\bullet-}$) has been investigated in a myriad of biological processes. Spin trapping coupled with electron paramagnetic resonance (EPR) is intensively used to characterize free radicals in biological milieu, with 5,5-dimethyl-1-pyrroline *N*-oxide (DMPO) being a popular spin trap for these studies. The formation of the spin adduct (DMPO−OOH) resulting from trapping superoxide with DMPO (Scheme 1) has been exploited to detect the generation of $O_2^{\bullet-}$ in a wide variety of biological and chemical systems.

* Address correspondence to this author. Phone: + 33 491 632 851. Fax: +33 491 288 758.

† Part of this work was presented at the annual meeting of the Royal Chemical Society ESR group (Warwick U.K., March 29, 2004).

‡ Laboratoire "Structure et Réactivité des Espèces Paramagnétiques" (SREP), CNRS and Aix-Marseille Universities.

§ Laboratoire de Chimie Théorique et Modélisation Moléculaire (LCT2M), CNRS and Aix-Marseille Universities.

|| Chemical Research Center, Institute for Chemistry.

(1) McCord, J. M.; Fridovich, I. *J. Biol. Chem.* **1969**, *244*, 6049−6055.

10.1021/jo048518z CCC: $30.25
Published on Web 01/13/2005

SCHEME 1

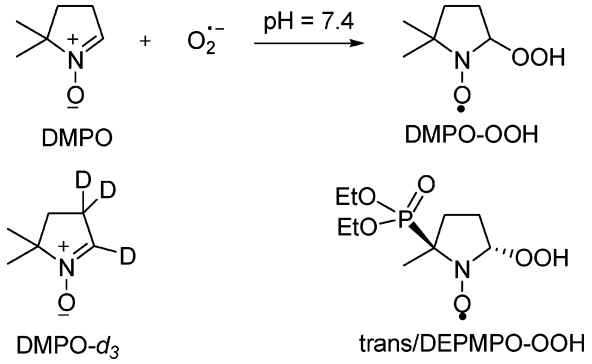

At 9.5 GHz, its 12-line EPR spectrum (Figure 1a) has been interpreted assuming that the lines resulted from the following couplings: $A_N \simeq 1.42$ mT, $A_{H^\beta} \simeq 1.134$ mT, and A_{H^γ} (1H) $\simeq 0.125$ mT. When the trapping of $O_2^{\bullet-}$ was performed with 5,5-dimethyl-[2,3,3-$^2H_3$]-1-pyrroline *N*-oxide (DMPO-d_3, Scheme 1), the EPR spectrum of the resulting spin adduct was composed of the expected triplet of triplets due to coupling of the unpaired electron with nitrogen and deuterium at carbon 2.[2] According to this result, the γ-coupling ($A_{H^\gamma} \simeq 0.125$ mT) observed for DMPO−OOH can be reasonably assigned to one of the hydrogen atoms bonded to carbon 3. Many examples of significant γ-couplings resulting from a W arrangement have been reported for nitroxides.[3] For the major conformers of DMPO−OOH, the ring puckering could result in a W arrangement involving a γ-hydrogen atom attached to carbon 3, thus explaining the γ-coupling.

The six doublets of the DMPO−OOH EPR spectrum exhibit a marked asymmetry which, considering a single species, cannot be reproduced by simulation without assuming chemical exchange between two conformers (Figure 1a).

Assuming that the 12-line signal of DMPO−OOH arises not from a γ-coupling but rather from the superimposition of two 6-line spectra belonging to equally populated, different conformers ***1*** and ***2*** with different line widths (***1***: $A_N = 1.425$ mT, $A_{H^\beta} = 1.245$ mT, $\Delta H_{pp} = 0.096$ mT. ***2***: $A_N = 1.425$ mT, $A_{H^\beta} = 1.01$ mT, $\Delta H_{pp} = 0.111$ mT), Buettner[4] showed that the asymmetrical DMPO−OOH spectrum could be reasonably reproduced. In 1995 we reported the synthesis of 5-(diethoxyphosphoryl)-5-methyl-1-pyrroline *N*-oxide (DEPMPO),[5] and we showed that it was much more convenient than DMPO for trapping $O_2^{\bullet-}$. The EPR spectrum of *trans*-DEPMPO−OOH (Scheme 1) exhibits a dramatic alternate line width which is nicely accounted for by the existence of a chemical exchange between two conformers.[5] Later, using various deuterated DEPMPOs, we clearly established[6] the existence of a set of γ-hyperfine splittings and assigned the largest coupling to one of the hydrogen atoms bonded to carbon 3 for both DEPMPO−OOH diastereoisomers. The alternate line width effect observed for the *trans*-DEPMPO−OOH was also observed for various DEPMPO−OOR (R = Me,[5] *n*-Bu,[7] *i*-Pr,[7] and *t*-Bu[6]) spin adducts. We thus considered[5] that the asymmetry of the DMPO−OOH spectrum could also result from a chemical exchange between two conformers $\boldsymbol{c_1}$ and $\boldsymbol{c_2}$, and indeed the spectrum was satisfactorily reproduced using an exchange rate $k_e = 1.5 \times 10^7$ s^{-1} and the following parameters: for $\boldsymbol{c_1}$, $A_N = 1.44$ mT, $A_{H^\beta} = 1.28$ mT, and $A_{H^\gamma} = 0.11$ mT; for $\boldsymbol{c_2}$, $A_N = 1.42$ mT, $A_{H^\beta} = 1.06$ mT, and $A_{H^\gamma} = 0.14$ mT.

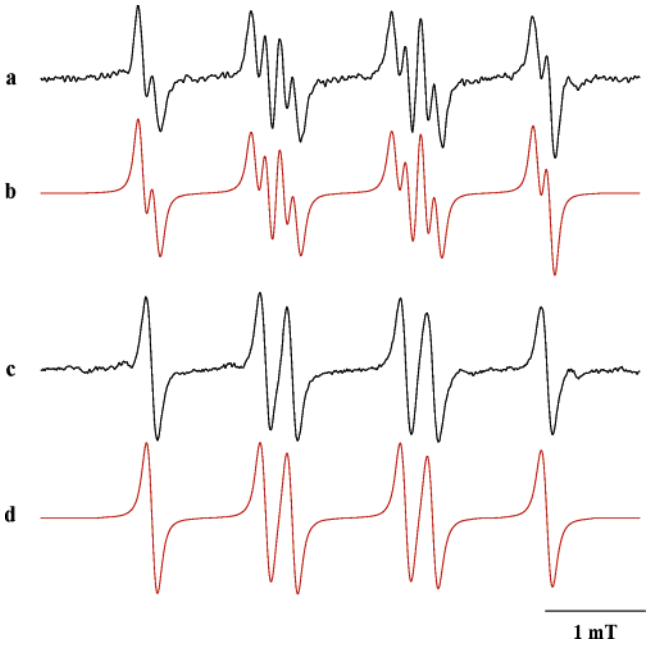

FIGURE 1. EPR spectra of DMPO and DMPO-d_2−superoxide spin adducts. (a) The incubation mixture contained hypoxanthin (0.2 mM), xanthin oxidase (0.05 U·mL^{-1}), DTPA (1 mM), and DMPO (100 mM) in phosphate buffer (0.1 M, pH 7.4). (b) Computer simulation of spectrum 1a, using the parameters reported in Table 2. (c) The incubation mixture contained hypoxanthin (0.2 mM), xanthin oxidase (0.05 U·mL^{-1}), DTPA (1 mM), and DMPO-d_2 (100 mM) in phosphate buffer (0.1 M, pH 7.4). (d) Computer simulation of spectrum 1c using the parameters reported in Table 2. Spectrometer settings: microwave power, 20 mW; modulation amplitude, 0.05 mT, time constant, 0.128 s; gain, 10^5; scan range, 6 mT; scan time, 82 s.

Recently, Rosen et al.[8] reexamined the assignment of the DMPO−OOH EPR spectrum. On the basis of the results of quantum mechanical calculations and EPR spectral modeling, Rosen et al. concluded that the spectrum is composed of two overlapping spectra arising from two independent conformers with the same A_N ($A_N = 1.377$ mT), different A_{H^β} ($A_{H^\beta} = 1.219$ and 0.978 mT), and no significant γ-couplings, as suggested first by Buettner. This conclusion is in contradiction with our assignments for the ESR spectra obtained by trapping $O_2^{\bullet-}$ with various pyrroline *N*-oxides.[5,9] However, many arguments used by Rosen et al. to reach their conclusion are questionable; hence, we decided to reexamine our previ-

(2) Pou, S.; Rosen, G. M.; Wu, Y.; Keana, J. F. W. *J. Org. Chem.* **1990**, *55*, 4438−4443.
(3) Ellinger, Y.; Subra, R.; Berthier, G. *J. Am. Chem. Soc.* **1978**, *100*, 4961−4963.
(4) Buettner, G. R. *Free Radical Res. Commun.* **1990**, *10*, 11−15.
(5) Fréjaville, C.; Karoui, H.; Tuccio, B.; Le Moigne, F.; Culcasi, M.; Pietri, S.; Lauricella, R.; Tordo, P. *J. Med. Chem.* **1995**, *38*, 258−65.
(6) Clément, J. L.; Finet, J. P.; Tordo, P. *Org. Biomol. Chem.* **2003**, *1*, 1591−1597.
(7) Karoui, H.; Tordo, P. Unpublished results.
(8) Rosen, G. M.; Beselman, A.; Tsai, P.; Pou, S.; Mailer, C.; Ichikawa, K.; Robinson, B. H.; Nielsen, R.; Halpern, H. J.; MacKerell, A. D., Jr. *J. Org. Chem.* **2004**, *69*, 1321−1330.

CHART 1

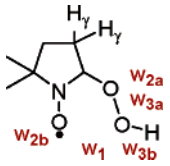

ous claim on the existence of a chemical exchange between two DMPO−OOH conformers.

Results and Discussion

1. Quantum-Mechanical Calculations. Quantum chemistry simulations have been performed in order to characterize the conformations of the DMPO−OOH adduct and also to compute the EPR isotropic hyperfine coupling constants (hcc's) according to the following equation:

$$A_i = \frac{8\pi}{3} g_e \beta_e g_i \beta_i \sum_{\mu,\nu} P^{\alpha-\beta}_{\mu\nu} \langle \phi_\mu | \delta(r) | \phi_\nu \rangle \qquad (1)$$

where g_e, g_i, β_e, β_i are the electron and nuclear gyromagnetic ratios and magnetons, respectively, h is the Planck constant, $P^{\alpha-\beta}$ is the spin density matrix expressed in the basis of the atomic orbitals φ, and $\delta(r)$ is the Dirac delta operator. The spin density matrix is evaluated according to the unrestricted Kohn−Sham method in density functional theory (DFT), using the hybrid three-parameter B3LYP functional[10] and the EPR-II basis set, developed by Barone and co-workers[11] for calculating the hcc's.

Since the EPR study of the DMPO−OOH spin adduct is performed in aqueous solution, one, two, or three close water molecules are included in the molecular model. For comparison, the nitroxide adduct is also modeled in a vacuum (model **0**). Five water complexes have been studied, always favoring the formation of hydrogen bonds.

Model **1**: one water molecule W_1 is added to the free DMPO−OOH adduct, approximately between the hydroperoxy group and the nitroxide oxygen atom.

Model **2a**: one water molecule W_{2a} is added to model **1**, approximately on the other side with respect to the hydroperoxy group.

Model **2b**: one water molecule W_{2b} is added to model **1**, approximately on the same side with respect to the hydroperoxy group.

Model **3a**: one water molecule W_{3a} is added to model **2b**, approximately on the other side with respect to the hydroperoxy group.

Model **3b**: one water molecule W_{3b} is added to model **2b**, after the hydrogen bond between a water molecule and the hydroperoxy group has been broken, rotating around the C_β−O bond.

All these models are summarized in Chart 1.

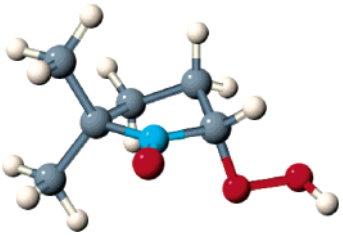

FIGURE 2. Structure of the DMPO−OOH adduct (model **0**).

Five-membered cycles are known to be very flexible; they present several local minima of similar energy that can be classified according to the notation introduced by Cremer and Pople.[12] If the DMPO−OOH adduct optimized in the vacuum adopts a ^{3}E conformation (Figure 2), the addition of a water molecule leads to a $^3T_4$ conformation that remains if other water molecules are added, except in the case of model **3b,** in which the cycle gets the E_4 conformation.

In model **1**, the water molecule W_1 establishes two strong hydrogen bonds with the nitroxide oxygen and the hydrogen of the hydroperoxyl group. Adding a second water molecule does not much affect the nitroxide structure: in one case (model **2a**), the water molecule W_{2a} only interacts with the hydroperoxy moiety; in the other one (model **2b**), the water molecule W_{2b} binds also to the oxygen atom of the nitroxide, albeit it takes place on the other face of the ring. This water network around the nitroxide moiety is consistent with the one found by Barone et al. for dimethylnitroxide.[13] On the other hand, it is also justified to find two hydroperoxy-bonded water molecules because it is known from Ar-matrix infrared spectroscopy studies of clusters[14] that the superoxide radical $O_2^{\bullet-}$ is hydrated by four water molecules and there is no reason the superoxide group (after the addition to the nitrone but before the protonation of the DMPO−O_2^- adduct) would lose all these water molecules. Then a third water molecule was added in order to combine the two previous models, **2a** and **2b**. In model **3a**, the hydrogen bonds are comparable to the ones found in the previous models. While in all these models the hydroperoxy hydrogen atom is directed toward the nitroxide side and the water molecules, it is interesting to study how the system evolves when this hydrogen atom points in the other direction. In model **3b**, the three water molecules form a large network, on the same side as the hydroperoxy group (Figure 3).

Hcc's are computed for each one of these structures according to eq 1. The results, expressed in mT, are reported in Table 1 , and experimental data are given for comparison. The largest variations involve the nitrogen atom, the β-hydrogen atom bonded to the carbon atom, and the oxygen atom of the hydroperoxy group directly connected to the nitroxide ring. With respect to the experimental hcc values, model **3b** seems to be the more realistic one, especially if the nitrogen hcc is corrected for the inaccuracy of the DFT-predicted A_N

(9) (a) Olive, G.; Mercier, A.; Le Moigne, F.; Rockenbauer, A.; Tordo, P. *Free Radical Biol. Med.* **2000**, *28*, 403−408. (b) Karoui, H.; Nsanzumuhire, C.; LeMoigne, F.; Tordo, P. *J. Org. Chem.* **1999**, *64*, 1471−1477. (c) Karoui, H.; Clément, J.-L.; Rockenbauer, A.; Siri, D.; Tordo, P. *Tetrahedron Lett.* **2004**, *45*, 149−152.

(10) Becke, A. D. *J. Chem. Phys.* **1993**, *98*, 5648−5652.

(11) Barone, V. In *Recent Advances in Density Functional Methods*, Part I; Chong, D. P., Ed.; World Scientific Publishing Co.: Singapore, 1996.

(12) Cremer, D.; Pople, J. A. *J. Am. Chem. Soc.* **1975**, *97*, 1354−1358.

(13) (a) Barone, V.; Bencini, A.; Cossi, M.; Di Matteo, A.; Mattesini, M.; Totti, F. *J. Am. Chem. Soc.* **1998**, *120*, 7069−7078. (b) Improta, R.; Barone, V. *Chem. Rev.* **2004**, *104*, 1231−1254.

(14) Weber, J. M.; Kelley, J. A.; Nielsen, S. B.; Ayotte, P.; Johnson, M. A. *Science* **2000**, *287*, 2461−2463.

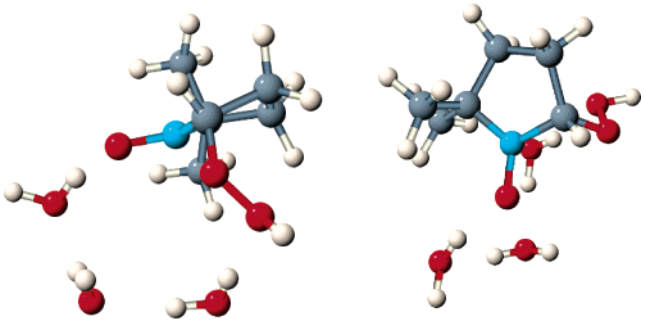

FIGURE 3. Structure of the (DMPO−OOH + 3 H_2O) complex (model **3b**).

TABLE 1. UB3LYP/EPR-II Computations of Isotropic Hyperfine Coupling Constants (in mT) for DMPO−OOH in a Vacuum and DMPO−OOH/Water Complexes

DMPO−OOH + $n H_2O$[a]	A_N	A_{H^β}	A_{H^γ} equatorial	A_{H^γ} axial	$A^{17}O$[b]
0	0.73	0.66	0.19	0.06	−1.53
1	0.95	0.93	0.19	0.10	−0.61
2a	0.93	1.04	0.18	0.12	−0.85
2b	1.04	0.82	0.20	0.10	−0.52
3a	1.02	0.99	0.18	0.12	−0.74
3b	1.04	1.11	0.17	0.03	−0.55
3b + PCM	1.08	1.16	0.18	0.02	−0.56
exp[c]	1.42	1.12	0.13		−0.59

[a] See text. [b] The hydroperoxyl oxygen atom directly connected to DMPO. [c] Mottley et al.[16]

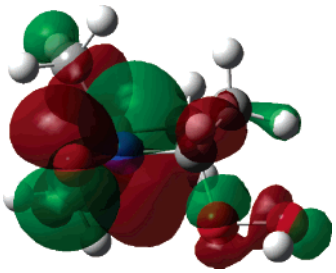

FIGURE 4. SOMO of DMPO−OOH (model **0**).

(between +0.2 and +0.4 mT).[13b] It is noteworthy that for all the models a significant positive coupling constant is predicted with the pseudoequatorial γ-hydrogen bonded to carbon 3. This coupling results from the delocalization of the unpaired electron as shown by the structure of the SOMO (Figure 4).

However, the theoretical models used in this study are still approximate. First, the influence of the bulk of the solvent has been neglected. It could be simulated using a continuum model.[15] However, as Barone has shown, the inclusion of some explicit water molecules in the model is a good starting point. Nevertheless, we checked the influence of the bulk solvent, imbedding the model **3b** in a continuum of dielectric constant 78.39. The corresponding hcc's are also reported in Table 1. One notes only small changes which do not modify the preceding conclusions. Second, solvation is a dynamic process and its treatment requires adapted tools, like

(15) (a) Rivail, J.-L.; Rinaldi, D. In *Computational Chemistry, Review of Current Trends*; Leszczynski, J., Ed.; World Scientific: New York, 1995. (b) Cramer, C. J.; Truhlar, D. G. *Chem. Rev.* **1999**, *99*, 2161−2200. (c) Tomasi, J.; Persico, M. *Chem. Rev.* **1994**, *94*, 2027−2094.

SCHEME 2. Synthetic Pathway for DMPO-d_2[a]

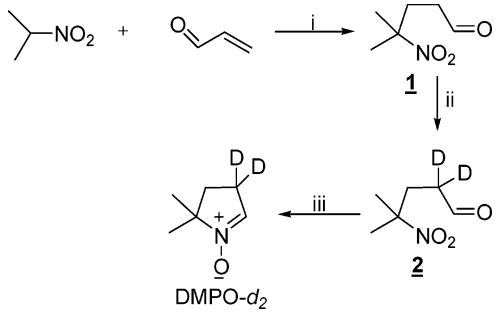

[a] (i) NEt_3 in CH_3CN, 3 d, RT, 46%; (ii) D_2O/pyridine, 30 h, RT, 23%; (iii) CH_3COOH/Zn in EtOH 95%, 15 °C, 21%.

molecular dynamics. We thus decided to prepare 5,5-dimethyl-[3,3-$^2H_2$]-1-pyrroline *N*-oxide (DMPO-d_2) and to generate the corresponding superoxide spin adduct DMPO-d_2−OOH. According to Rosen's conclusion, the EPR spectra of DMPO−OOH and DMPO-d_2−OOH should be identical. However, if a γ-coupling with a hydrogen bonded to carbon 3 contributes to the pattern of the DMPO−OOH spectrum, the DMPO-d_2−OOH spin adduct will exhibit a six-line spectrum.

2. Spin Trapping Studies. DMPO-d_2 was obtained from γ-nitroaldehyde **2**, via the reduction procedure described by Haire et al. (Scheme 2).[17] H−D exchange in the α position of the aldehyde function of **1** was carried out in a D_2O/pyridine mixture.[18]

(a) Spin Trapping of Superoxide Anion and *tert*-Butylperoxyl Radicals. Spin trapping of superoxide with DMPO (Figure 1a) and DMPO-d_2 (Figure 1c) was performed at pH 7.4 using a hypoxathin (HX; 0.2 mM)/xanthin oxidase (XOD; 0.05 U·mL^{-1}) superoxide-generating system. The same signals were observed by adding a DMSO solution of KO_2 (0.1 M) in the presence of 1 equiv of 18C6 in phosphate buffer (0.1 M, pH 7.4; data not shown). The ESR spectra were abolished in the presence of SOD (1500 U·mL^{-1}), proving that the signal can be unambiguously assigned to DMPO−OOH and DMPO-d_2−OOH spin adducts. In the presence of glutathione peroxidase (10 U·mL^{-1}) and glutathione (0.5 mM) in the previous incubation mixture, only the DMPO-d_2−OH spin adduct (A_N = 1.498 mT, A_{H^β} = 1.485 mT) was observed (data not shown). *Tert*-butylperoxyl (*t*-BuOO•) and *tert*-butoxyl (*t*-BuO•) radical trappings were performed by irradiating a toluene solution of *t*-BuOOH (1.5 M) or *t*-BuO*t*-Bu (0.5 M) in the presence of DMPO or DMPO-d_2 (0.1 M), respectively.

The spectrum of DMPO-d_2−OOH (Figure 1c) is composed of only six lines. This result establishes unambiguously that a γ-H splitting (H bonded to carbon 3) contributes to the pattern of the DMPO−OOH spectrum. The same conclusion was reached for the spectra[19] of DMPO−OO*t*-Bu and DMPO−O*t*-Bu (Table 2).

(b) Calculation of EPR Spectra. Two alternative models were considered to calculate the DMPO−OOR

(16) Mottley, C.; Connor, H. D.; Mason, R. P. *Biochem. Biophys. Res. Commun.* **1986**, *141*, 622−628.
(17) Haire, D. L.; Hilborm, J. W.; Janzen, E. G. *J. Org. Chem.* **1986**, *51*, 4298−4300.
(18) Tucker, W. P.; Tove, S. B.; Kepler, C. R. *J. Labelled Compd. Radiopharm.* **1971**, *7*, 137−143.
(19) Davies, M. J.; Slater, T. F. *Biochem. J.* **1986**, *240*, 789−795.

TABLE 2. EPR Coupling Constants for DMPO and DMPO-d_2 Spin Adducts

spin adduct	source	solvent	population[a]/%	A_N/mT	A_{H^β}/mT	A_{H^γ}/mT	A_{D^γ}/mT	k^b/($\times 10^{-7}$ s)
DMPO−OOH	HX/XO	water[c]	67	1.415	1.134	0.158		4.17
			33	1.409	1.178	0.017		4.17
DMPO-d_2−OOH	HX/XO	water[c]	67	1.415	1.134		0.024	4.17
			33	1.409	1.178		0.003	4.17
DMPO−OO*t*-Bu	*t*-BuOOH/$h\nu$	toluene	60	1.295	0.931	0.211		32.26
			40	1.298	0.971	0.070		32.26
DMPO-d_2−OO*t*-Bu	*t*-BuOOH/$h\nu$	toluene	60	1.295	0.931		0.032	32.26
			40	1.298	0.971		0.010	32.26
DMPO−O*t*-Bu	(*t*-BuO)$_2$/$h\nu$	toluene	100	1.309	0.749	0.182		
DMPO-d_2−O*t*-Bu	(*t*-BuO)$_2$/$h\nu$	toluene	100	1.309	0.749		0.028	

[a] Population of each conformer. [b] Exchange rate. [c] 0.1 M phosphate buffer, pH 7.4.

and DMPO-d_2−OOR spectra (R = H, *t*-Bu). Model **A** is essentially the model suggested by Rosen et al.:[8] two exchanging DMPO−OOH conformers with no A_{H^γ} and different A_N and A_{H^β}. In model **B** we considered two exchanging conformers with different A_N, A_{H^β}, and A_{H^γ}.

When the rate of exchange is infinitely slow relative to the EPR time scale, model **A** offers a good fit with a regression of 0.98496. When the EPR spectra of the two conformers are superimposed, the major conformer (52%) has the β-coupling 1.261 mT, the minor conformer has the β-coupling 1.017 mT, and half of the difference (0.122 mT) between the two indeed reproduces an apparent "γ-splitting". In the case of model **B**, the regression is increased to 0.98651, and the improvement of regression, 0.00155, is larger than the criteria of significance, 0.00064, computed from the noise of the spectrum.[20] Consequently, model **B** offers a significantly better fit than model **A**. In model **B**, A_{H^β} was found to be nearly the same in the two exchanging conformers: 1.134 versus 1.178 mT; however, A_{H^γ} is significantly different (ΔA_{H^γ} = 0.14 mT), and this difference causes the spectrum asymmetry. The deuteration gives the most clear-cut evidence for model **B**; while for model **A** only a slight variation of line width is expected as a consequence of deuteration, model **B** agrees with the observed six-line spectrum (Figure 1c and d). If we replace A_{H^γ} by $A_{D^\gamma} = 0.153A_{H^\gamma}$, keeping constant all the other parameters calculated for DMPO−OOH, model **B** reproduces very well the spectrum recorded for DMPO-d_2−OOH.

It is worthy of note that, as expected for a chemical exchange between two conformers with small differences in their coupling constants (ΔA_{D^γ} = 0.021 mT, ΔA_{H^β} = 0.044 mT), the lines of the DMPO-d_2−OOH spectrum do not show any significant asymmetry.

The DMPO−OO*t*-Bu EPR spectrum recorded in toluene has a much less marked asymmetry than that observed for DMPO−OOH in water solution; nevertheless, only model **B** could offer an adequate fit for the calculated spectra of DMPO−OO*t*-Bu and DMPO-d_2−OO*t*-Bu.

Conclusion

The six-line EPR spectrum observed for the superoxide adduct of 5,5-dimethyl-[3,3-$^2H_2$]-1-pyrroline *N*-oxide (DMPO-d_2−OOH) establishes unambiguously that a γ-splitting arising from a hydrogen atom bonded to carbon 3 contributes to the 12-line spectrum of DMPO−OOH. The same conclusion was reached for the DMPO−OO*t*-Bu and DMPO−O*t*-Bu spin adducts. For DMPO−OOH, DFT calculations including a water network around the nitroxide moiety confirm the existence of a significant coupling (≃0.2 mT) with the pseudoequatorial hydrogen bonded to carbon 3 of the pyrroline ring. The asymmetry of the DMPO−OOH spectrum can be nicely reproduced considering a two-site chemical exchange and assuming that the sites correspond to two DMPO−OOH conformers exhibiting different γ-splitting. However, each site could also correspond to various DMPO−OOH conformers interconverting rapidly; the coupling constant values reported in Table 2 would then correspond to average values. Further studies are needed to determine the complete conformational behavior of DMPO−OOH in water solution. A good compromise to address this point would be the use of the hybrid quantum-mechanical/molecular-mechanical methods:[21] the nitroxide and some close water molecules are treated quantum-mechanically while the rest of the solvent is treated classically.

Experimental Section

1. Quantum-Mechanical Computations. Quantum-mechanical studies were performed with the Gaussian03 package.[22] Density functional theory calculations were achieved thanks to the unrestricted Kohn−Sham method, using the hybrid three-parameter B3LYP functional[10] and the EPR-II basis set, developed by Barone and co-workers[11] for calculating hyperfine coupling constants. The molecular geometry was first fully optimized to a minimum on the potential energy surface (harmonic frequencies are checked to be all positive) using the 6-31G(d) basis set, and then it was reoptimized using

(20) Rockenbauer, A.; Szabó-Plánka, T.; Árkosi, Z.; Korecz, L. *J. Am. Chem. Soc.* **2001**, *123*, 7646−7654.

(21) (a) Warshel, A.; Levitt, M. *J. Mol. Biol.* **1976**, *103*, 227−249. (b) Field, M. J.; Bash, P. A.; Karplus, M. *J. Comput. Chem.* **1990**, *11*, 700−733. (c) Gao, J. In *Reviews in Computational Chemistry*; Lipkowitz, K. B., Boyd, D. B., Eds.; VCH Publishers: New York, 1995. (d) Monard, G.; Merz, K. M., Jr. *Acc. Chem. Res.* **1999**, *32*, 904−911.

(22) Frisch, M. J.; Trucks, G. W.; Schlegel, H. B.; Scuseria, G. E.; Robb, M. A.; Cheeseman, J. R.; Montgomery, J. A., Jr.; Vreven, T.; Kudin, K. N.; Burant, J. C.; Millam, J. M.; Iyengar, S. S.; Tomasi, J.; Barone, V.; Mennucci, B.; Cossi, M.; Scalmani, G.; Rega, N.; Petersson, G. A.; Nakatsuji, H.; Hada, M.; Ehara, M.; Toyota, K.; Fukuda, R.; Hasegawa, J.; Ishida, M.; Nakajima, T.; Honda, Y.; Kitao, O.; Nakai, H.; Klene, M.; Li, X.; Knox, J. E.; Hratchian, H. P.; Cross, J. B.; Adamo, C.; Jaramillo, J.; Gomperts, R.; Stratmann, R. E.; Yazyev, O.; Austin, A. J.; Cammi, R.; Pomelli, C.; Ochterski, J. W.; Ayala, P. Y.; Morokuma, K.; Voth, G. A.; Salvador, P.; Dannenberg, J. J.; Zakrzewski, V. G.; Dapprich, S.; Daniels, A. D.; Strain, M. C.; Farkas, O.; Malick, D. K.; Rabuck, A. D.; Raghavachari, K.; Foresman, J. B.; Ortiz, J. V.; Cui, Q.; Baboul, A. G.; Clifford, S.; Cioslowski, J.; Stefanov, B. B.; Liu, G.; Liashenko, A.; Piskorz, P.; Komaromi, I.; Martin, R. L.; Fox, D. J.; Keith, T.; Al-Laham, M. A.; Peng, C. Y.; Nanayakkara, A.; Challacombe, M.; Gill, P. M. W.; Johnson, B.; Chen, W.; Wong, M. W.; Gonzalez, C.; Pople, J. A. *Gaussian 03*, Revision B.3; Gaussian, Inc.: Pittsburgh, PA, 2003.

the EPR-II basis set, for which hcc's are calculated. Since we are not interested in energetics, the results are not corrected for basis set superposition error. In all the calculations, the spin contamination is negligible ($\langle S^2 \rangle < 0.76$). The bulk solvent calculation is performed using the polarizable continuum method (PCM). The molecular cavity is built using the UFF radii of all the atoms. A single point calculation is made on the geometry optimized in vacuo.

2. Chemicals. All chemicals and organic solvents were commercially available and used without further purification. ^{1}H NMR and ^{13}C NMR spectra were recorded at 300 or 200 MHz and 75.47 or 50.32 MHz, respectively. Chemical shifts (δ) are reported in ppm for solutions in $CDCl_3$, with Me_4Si as an internal reference and J values given in Hz.

3. Analysis of Deuteration. The decrease of the intensities of the ^{1}H NMR signal of exchanging protons has been considered as a probe for exchanging rate. Quantitative estimations were carried out by comparing nonexchanging proton signal intensities with those of exchanging protons. The isotopic purity was considered as sufficient (estimated > 95%) when exchanging proton signals disappeared on the ^{1}H NMR spectrum.

(a) Synthesis of 4-Methyl-4-nitropentanal (1). Triethylamine (2 mL) was slowly added at 0 °C to a mixture of freshly distilled acroleine (20 g, 0.35 mol) and 2-nitropropane (17.8 g, 0.2 mol) in CH_3CN (100 mL). The mixture was then stirred for 3 days at RT. The mixture was concentrated under vacuum, and distillation under reduced pressure (62−64 °C, 0.1 mmHg) afforded a colorless oil (10.5 g, 46%). ^{1}H NMR (300 MHz, $CDCl_3$): δ 1.60 (s, 6H), 2.25 (t, J = 9.0 Hz, 2H), 2.52 (t, J = 9.0 Hz, 2H), 9.78 (s, 1H). ^{13}C NMR (75.47 MHz, $CDCl_3$): δ 25.61, 32.09, 38.60, 87.09, 199.68.

(b) Synthesis of 4-Methyl-4-nitro-[2,2-$^2H_2$]-pentanal (2). 4-methyl-4-nitropentanal (5.5 g, 37.9 mmol) was stirred at RT in D_2O (40 mL) and dry pyridine (40 mL) for 30 h. The isotopic purity was considered as sufficient (estimated > 95%) when the NMR signals of the exchanging protons disappeared. The resulting mixture was carefully acidified at 0 °C with H_2SO_4 until pH 1 and extracted with Et_2O (3 × 20 mL). The combined organic phases were dried over $MgSO_4$, filtered off, and evaporated under vacuum. Distillation under reduced pressure (62−64 °C, 0.1 mmHg) afforded a colorless oil (1.3 g, 23%). ^{1}H NMR (300 MHz, $CDCl_3$): δ 1.60 (s, 6H), 2.23 (s, 2H), 9.78 (s, 1H). ^{13}C NMR (75.47 MHz, $CDCl_3$): δ 25.8, 32.1, 38.0 (m, J_{CD} = 18.9 Hz), 87.1, 199.9.

(c) Synthesis of 5,5-Dimethyl-[3,3-$^2H_2$]-1-pyrroline *N*-Oxide (DMPO-d_2). Acetic acid was added to a stirred solution of 4-methyl-4-nitro-[2,2-$^2H_2$]-pentanal (1.3 g, 8.84 mmol) and Zn dust (1.58 g, 24.15 mmol) in 95% EtOH (27 mL) at 15 °C until complete disappearance of the starting material (followed by TLC). The mixture was stirred at 15 °C another 2 h, and CH_2Cl_2 (20 mL) was then added. The mixture was filtered off and concentrated under vacuum. D_2O (40 mL) was added, and the aqueous phase was extracted with pentane (3 × 10 mL), saturated by NaCl, and extracted thoroughly with $CHCl_3$ (4 × 20 mL). The combined organic phases were dried over $MgSO_4$ and evaporated under vacuum. Distillation under reduced pressure (60 °C, 0.1 mmHg) afforded the pure nitrone as a colorless oil which solidified at low temperature (0.21 g, 21%). ^{1}H NMR (300 MHz, $CDCl_3$): δ 1.43 (s, 6H), 2.12 (s, 2H), 6.79 (s, 1H). ^{13}C NMR (75.47 MHz, $CDCl_3$): δ 23.5 (m, J_{CD} = 20.35 Hz), 25.2, 33.7, 73.3, 131.5.

(d) Spin Trapping Studies. Xanthine oxidase (XOD), bovine erythrocyte superoxide dismutase (SOD), glutathione (GSH), glutathione peroxidase (Gpx), diethylenetriaminepentaacetic acid (DTPA), di-*tert*-butylperoxide, *tert*-butylhydroperoxide, and other chemicals were purchased from commercial suppliers.

4. ESR Measurements. ESR spectra were recorded at room temperature using an X-band spectrometer at 9.5 GHz employing 100 kHz field modulation. Reaction mixtures were prepared in a chelex-treated phosphate buffer (0.1 M, pH 7.4). ESR spectra were simulated using ESR software developed by D. Duling, from the Laboratory of Molecular Biophysics, NIEHS, USA,[23] and by A. Rockenbauer, from the Central Research Institute of Chemistry, Hungary.[24] The UV photolysis was performed by a 300 W xenon−mercury lamp.

5. Superoxide Trapping—Hypoxanthine/Xanthine Oxidase System. Xanthine oxidase (0.05 U·mL^{-1}) was added to a solution of DMPO and DMPO-d_2 (0.1 M), DTPA (0.5 mM), and hypoxanthine (0.2 mM) in phosphate buffer (0.1 M, pH 7.4). The ESR spectrum was recorded 60 s after the addition of XOD.

6. HO$^\bullet$ Trapping—Fenton System. Hydroxyl radical was generated by adding $FeSO_4$ (0.5 mM) to a solution of DMPO or DMPO-d_2 (25 mM) and H_2O_2 (2 mM) in phosphate buffer (0.1 M, pH 7.4). The ESR spectrum of the hydroxyl adduct was recorded 60 s after addition of ferrous sulfate.

7. *t*-BuOO$^\bullet$ Radical Trapping. *t*-BuOO$^\bullet$ was produced by UV photolysis of a solution of *tert*-butyl hydroperoxide (1.5 M) and DMPO and DMPO-d_2 (0.1 M) in toluene.

8. *t*-BuO$^\bullet$ Radical Trapping. *t*-BuO$^\bullet$ was generated by UV photolysis of a solution of di-*tert*-butylperoxide (0.5 M) and DMPO or DMPO-d_2 (0.1 M) in toluene.

Acknowledgment. The authors acknowledge the CNRS, the University of Provence, and the Hungarian Research Fund (Grant OTKA T046953) for their financial support.

JO048518Z

(23) This software is available via the World Wide Web at http://EPR.niehs.nih.gov/PEST.html.

(24) Rockenbauer, A.; Korecz, L. *Appl. Magn. Reson.* **1996**, *10*, 29-43.